Extended Analysis of the Spectrum and Term System of Be III

Physica Scripta. Vol. 64, 566–572, 2001

Extended Analysis of the Spectrum and Term System of Be III

C. Jupén[1], A. Meigs[2], M. von Hellermann[3], H. W. Morsi[4], M. Beringer[2], S. Mannervik[5] and I. Martinson[1]

[1]Department of Physics, Lund University, Box 118, SE-221 00 Lund, Sweden
[2]UKAEA/Euratom Fusion Association, Culham Science Centre, Abingdon, Oxon, OX14 3DB, UK
[3]Forschungszentrum Jülich GmbH, D-53425 Jülich, Germany
[4]Commission of the European Communities, DGXI I, Brussels, Belgium
[5]Atomic Physics, Stockholm University, SE-104 05 Stockholm, Sweden

Received July 5, 2001; accepted in revised form July 16, 2001

PACS Ref: 32.30.-r, 32.30.Jc

Abstract

We report an extended and partly revised analysis of doubly ionized beryllium, Be III. Spectra of Be were recorded at the JET fusion facility where beryllium was used as surface material in the divertor. Observations of the divertor plasma have revealed many previously unknown Be lines, of which 28 (in the range 2100–5300 Å) have been classified as Be III transitions. We have also reanalyzed beam-foil spectra of Be (1900–5500 Å), recorded during a study of inner-shell excited levels in Be II. This yielded 7 additional Be III lines. These data, together with 32 previously known lines now represent an observed term system comprising 46 levels, with relative energy value uncertainties of around 1 cm^{-1}. The ionization energy of $1s^2\,{}^1S$ has been determined to $1\,241\,243.5 \pm 14$ cm^{-1} with an estimated Lamb shift of -43 ± 14 cm^{-1}. A complete description of the term scheme deduced from polarization and Ritz formulae is presented.

1. Introduction

In their important study of the He I-like spectrum CV. Edlén and Löfstrand [1] in 1970 pointed out that of the two-electron spectra (He isoelectronic sequence) only He I and Li II were thoroughly known from the experimental point of view. Substantial progress has been made in the following years, however, and fairly extensive experimental data are now available for Be III [2,3], B IV [4], C V [1,5], N VI [6] and O VII [7], whereas the data are quite limited for higher ionization stages [8].

Experimental studies of the structure of He-like ions are of great interest for atomic theory, where modern theoretical calculations, e.g. those by Drake [9,10] and Cheng *et al.* [11] are characterized by very high accuracy. Furthermore, it is well known that comparisons between theoretical and experimental data provide detailed information about QED effects in two-electron spectra.

In the present paper we report a study of Be III transitions in the range 2000–5500 Å. The experimental work was carried out at the JET tokamak where in 1994/95 beryllium was used as surface material in the pumped divertor. The Be ions in the plasma were excited by charge-exchange processes. However, we also used beam–foil (BF) spectra of Be, recorded in 1980 at the Research Institute of Physics (now the Manne Siegbahn Laboratory) in Stockholm. Spectra obtained by these two techniques show similarities but also differences (e.g. the production of doubly-excited states is favored in the BF case). Thus, the different spectra complement each other.

2. Previous spectroscopic analyses of Be III

The Be III resonance lines $1s^2\ {}^1S - 1snp\ {}^1P$ ($n = 2$–7) were established already in the 1930s [12–16] by means of open spark light sources. The experimental wavelength uncertainties of these XUV lines (in the 80–100 Å region) varied from 0.003–0.01 Å. A significant improvement was made by Svensson [17] by the remeasurement of the $1s^2\,{}^1S$–$1s2p\,{}^1P$ transition, yielding a value of 100.2552 ± 0.0015 Å, corresponding to ± 15 cm^{-1} in wavenumber uncertainty. The reduced uncertainty made it possible to achieve an ionization energy which is comparable with accurate theories.

In more recent work, Eidelsberg [2] and Löfstrand [3], investigated the Be spectra up to 6200 Å. Together with the earlier results [12–17] about 30 Be III lines were thereafter established. However, the number of observed transitions above 2000 Å was quite limited. The experimental term system [3] that included 25 levels, up to $n = 5$, was built on theoretical values [18] of the $1s2p\,{}^1P$ and ${}^3P$ energies, in order to increase the accuracy.

In recent years extremely accurate remeasurements of the $1s2s\,{}^1S$–$1s2p\,{}^1P$ and $1s2s\ {}^3S$–$1s2p\,{}^3P$ multiplets have been reported, based on the fast-ion-beam laser technique [19,20]. Uncertainties as low as 10^{-8} were thereby obtained, see Ref. [20].

3. Experiment and results

The new spectral data have been obtained by using the charge-exchange spectroscopy diagnostics at JET [21]. A characteristic process is here $Be^{3+}(1s) + H(2s) \rightarrow Be^{2+}(1s5l) + H^+$. This state-selective process has a large cross section at low energies (1–100 eV) which are typical in the divertor region. The divertor spectra were analyzed with two Czerny-Turner spectrometers which together covered the wavelength region 2000–8000 Å. More details about the experimental conditions are given in Ref. [22].

All spectra were analyzed using the Gaussian deconvolution program Gfit [23]. As in the Be II investigation [22] the wavelength scale was determined using reference lines, i.e. well-known transitions in Be I, Be III, C II–C IV and N II-N IV, also emitted from the divertor plasma. The BF spectra now used were recorded for a study of the doubly excited quartet levels $1s2snl$ and $1s2pnl\ {}^4L$ in Be II. See Ref. [24] where a Be beam-foil spectrum is displayed and details are given about the experiment and data analyses.

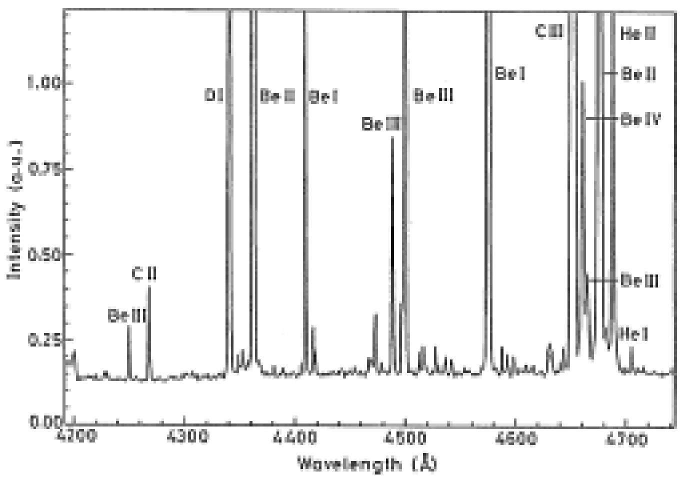

Fig. 1. Spectrum from 4200 to 4750 Å recorded at JET.

An example of a JET spectrum between 4200 and 4750 Å is shown in Fig. 1. The Be III lines close to 4500 Å have been identified as 4d ^{3}D–5f ^{3}F, 4d ^{1}D–5f ^{1}F and 4f–5g combinations, at 4486.52, 4495.57 and 4497.98 Å respectively. Their appreciable intensities are a consequence of the selective charge-exchange process.

Using the JET data we have classified 28 Be III transitions in the wavelength range 2130–5300 Å which have not been reported earlier [2,3]. Most of these new lines also appear in the beam–foil spectra. However, the latter exhibit additional transitions which were not observed in JET spectra, mainly because of masking and blends from some plasma impurities. All new lines are listed in Table I together with previous experimental data. Nearly 70 Be III transitions between singly-excited levels of the 1s*nl* ^1L or ^3L are now known. Moreover, there are also experimental data for the doubly-excited Be III system 2s*nl* and 2p*nl* [25], obtained by means of beam-foil spectroscopy, but these will not be dealt with in the present paper.

4. Analysis

4.1. *The observed term system*

A crucial factor in the analysis of the spectra of He-like ions (as well as of other sytems with two valence electrons) is to find the intersystem lines that connect the singlet and triplet term systems. In the Be III case the identification in early JET spectra of the 1s^2 ^{1}S$_0$–1s2p ^{3}P$_1$ intercombination line at 101.695 ± 0.015 Å [26] is therefore of great value, despite the fact that the accuracy is somewhat modest. However, this transition complements the observation of the 1s^2 ^{1}S–*n*p ^{1}P series where the 1s^2 ^{1}S–1s2p ^{1}P line at 100.252±0.0015 Å is crucial for determination of the absolute term system accuracy. It is interesting to note that the intersystem transition was not observed earlier for Be III, although it is well known in C V, and O VII, for instance.

Other combinations between the two systems have been realized by the observed *n*d ^{1}D–*n*f ^{1,3}F transitions with unresolved singlet and triplet states, thus making them indirectly connected. The singlet and triplet splittings of the *n*f F ($n = 4$–7) terms are theoretically predicted to be less than 0.5 cm^{-1} which lie within the experimental uncertainties of the present work. In order to build up the observed term system an iterative procedure was applied, using the computer code ELCALC [27]. As input values we used the uncertainties of the observed wavelengths (Table I) as weighting factors in a least squares fitting procedure. For the lines used in this fit calculated wavelengths as well as the differences between observed and calculated values are given in Table I. These figures are thus measures of reliability of the identified lines. With the aid of this iteration method 8 lines identified by Eidelsberg [2], but discarded by Löfstrand [3], have been included in the line list. With the exception of the 3d ^{3}D–5f ^{3}F and 3d ^{3}D–5p ^{3}P combinations which lie outside the stated error bars, but within two standard deviations, all transitions fit well into the system. The extended term system now includes all triplet and singlet levels from $n = 2$ up to $n = 7$. It should be noted that the important $n = 6$ levels, 6s ^{1}S, 6s ^{3}S, 6d ^{1}D and 6d ^{3}D, were established from BF spectra. However, the triplet structure could be resolved only for the 2p ^{3}P term. In Table II we have listed all experimental energy level values with their relative uncertainties. The number of combinations for each level is also included. The other two columns give the deviations from level values calculated with the Ritz formalism, to be outlined in the next section. An energy level diagram is shown in Fig. 2.

4.2. *The ionization limit*

4.2.1. *The Ritz formulae.* Another consistency check of the derived experimental energy level system is provided by the Ritz formula, see Edlén [28], which takes advantage of the regularities of the series members. The formula expresses the quantum defect δ ($\delta = n - n^*$), as a function of the reduced term value t ($t = T/R\zeta^2$) and can be written as:

$$\delta = a + bt + ct^2. \quad (2)$$

For Be the value of the Rydberg constant R_{Be} is 109 730.63 cm^{-1}. The parameters to be fitted are thus the term value (T) and coefficients a, b and c. In He-like spectra a smooth behaviour is expected for each spectral series. There are essentially two ways to determine the ionization limit, either to establish an ionization limit for each observed singlet and triplet branch of the lsnl series, with subsequent averaging,

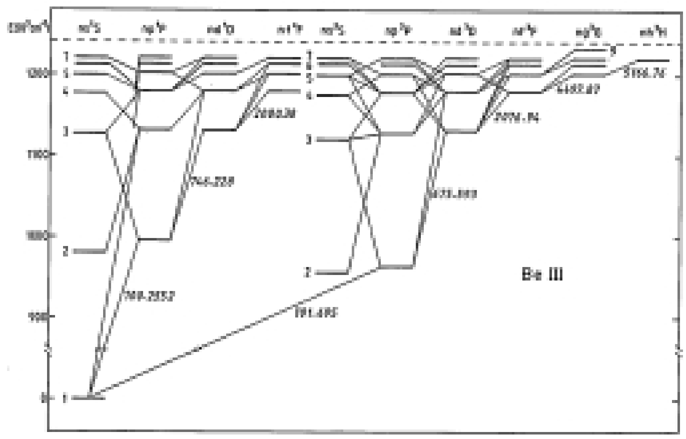

Fig. 2. Energy level diagram of Be III.

Table I. *Observed Be III transitions. (Wavelengths in Å).*

λ_{obs}	Uncertainty	Ref.	λ_{calc}	$\Delta\lambda_{obs\text{-}calc}$ [c]	Transition
81.891	0.004	15			$1s^2\ ^1S$–$7p\ ^1P$
82.377	0.004	15			$1s^2\ ^1S$–$6p\ ^1P$
83.202	0.003	15	83.200	0.002	$1s^2\ ^1S$–$5p\ ^1P$
84.750	0.010	13	84.754	−0.004	$1s^2\ ^1S$–$4p\ ^1P$
88.308	0.005	13	88.309	−0.001	$1s^2\ ^1S$–$3p\ ^1P$
100.2552	0.0015	13	100.2552	0.000	$1s^2\ ^1S$–$2p\ ^1P$
101.695	0.015	26	101.692	0.003	$1s^2\ ^1S$–$2p\ ^3P$
509.99	0.02	3	509.98	0.01	$2p\ ^3P$–$4d^3D$
549.310	0.03	3	549.311	−0.001	$2p\ ^1P$–$4d\ ^1D$
582.078	0.01	3	582.084	−0.006	$2s\ ^3S$–$3p\ ^3P$
661.322	0.01	3	661.300	0.022	$2s\ ^1S$–$3p\ ^1P$
675.593	0.008	3	675.617	−0.024	$2p\ ^3P$–$3d\ ^3D$
725.586	0.011	3	725.595	−0.009	$2p\ ^3P$–$3s\ ^3S$
746.228	0.008	3	746.231	−0.003	$2p\ ^1P$–$3d\ ^1D$
767.75	0.03	2			$2p\ ^1P$–$3s\ ^1S$
1114.69	0.05	2	1114.76	−0.07	$3d\ ^3D$–$7f$
1213.12	0.05	2	1213.15	−0.03	$3d\ ^3D$–$6f$
1214.32	0.05	2	1214.30	0.02	$3d\ ^1D$–$6f$
1362.25	0.05	2	1362.37	−0.12	$3p\ ^3P$–$5d^3D$
1421.26	0.05	2	1421.34	−0.08	$3d\ ^3D$–$5f$
1422.86	0.05	2	1422.92	−0.06	$3d\ ^1D$–$5f$
1435.17	0.05	2	1435.27	−0.10	$3d\ ^3D$–$5p\ ^3P$
1754.69	0.03	3	1754.71	−0.02	$3s\ ^3S$–$4p\ ^3P$
1954.97	0.03	3	1954.96	0.01	$3p\ ^3P$–$4d\ ^3D$
2076.94	0.02	3	2076.96	−0.02	$3d\ ^3D$–$4f$
2080.38	0.02	3	2080.33	0.05	$3d\ ^1D$–$4f$
2122.27	0.04	3	2122.22	0.05	$3p\ ^1P$–$4d\ ^1D$
2127.20	0.04	3	2127.18	0.02	$3p\ ^3P$–$4s\ ^3S$
2136.51	0.15		2136.32	0.19	$3d\ ^3D$–$4p\ ^3P$
2195.48[a]	0.30		2195.41[b]	0.07	$3p\ ^1P$–$4s\ ^1S$
2330.25	0.15		2330.28	−0.03	$4p\ ^3P$–$7d\ ^3D$
2371.62	0.15		2371.64	−0.02	$4p\ ^3P$–$7s\ ^3S$
2401.29	0.15		2401.24	0.05	$4d\ ^3D$–$7f$
2404.69 bl	0.30				$4f$–$7g$
2415.75	0.15		2415.58	0.17	$4d\ ^3D$–$7p\ ^3P$
2426.43	0.15		2426.43	0.00	$4p\ ^1P$–$7d\ ^1D$
2807.08[a]	0.20		2807.04[b]	0.04	$4p\ ^3P$–$6d\ ^3D$
2904.69[a]	0.30		2904.66[b]	0.03	$4p\ ^3P$–$6s\ ^3S$
2909.76	0.15		2909.80	−0.04	$4d\ ^3D$–$6f\ ^3F$
2913.60	0.15		2913.62	0.06	$4d\ ^1D$–$6f\ ^1F$
2914.91 bl	0.30				$4f$–$6g$
2943.80[a]	0.60		2943.71[b]	0.09	$4d\ ^3D$–$6p\ ^3P$
2946.95[a]	0.40		2947.23[b]	−0.28	$4p\ ^1P$–$6d\ ^1D$
2987.85[a]	0.60		2987.99[b]	−0.14	$4p\ ^1P$–$6s\ ^1S$
3660.09[a]	0.50		3660.02b[a]	0.07	$5f$–$9g$
3720.85	0.03	3	3720.86	−0.01	$2s\ ^3S$–$2p\ ^3P_2$
3720.8486	0.00004	20			
3721.31	0.03	3	3721.32	−0.01	$2s\ ^3S$–$2p\ ^3P_0$
3721.3106	0.00005	20			
3722.91	0.03	3	3722.92	−0.01	$2s\ ^3S$–$2p\ ^3P_1$
3722.9124	0.00004	20			
3881.53	0.20		3881.43	0.10	$4s\ ^3S$–$5p\ ^3P$
4249.14	0.10	3	4249.07	0.07	$4p\ ^3P$–$5d\ ^3D$
4458.22	0.20		4458.27	−0.05	$4d\ ^1D$–$5p\ ^1P$
4486.52	0.15		4486.51	0.01	$4d\ ^3D$–$5f\ ^3F$
4495.57	0.15		4495.40	0.17	$4d\ ^1D$–$5f\ ^1F$
4497.98	0.15				$4f$-$5g$
4505.13	0.15		4505.12	0.01	$4f\ ^3F$–$5d\ ^3D$
4575.47	0.20				$4p\ ^1P$–$5d\ ^1D$
4628.29	0.20		4628.27	0.02	$4d\ ^3D$–$5p\ ^3P$
4663.33	0.20		4663.45	−0.12	$4p\ ^3P$–$5s\ ^3S$
4709.68	0.20		4709.79	−0.11	$5s\ ^3S$–$7p\ ^3P$
4750.34	0.20				$4p\ ^1P$–$5s\ ^1S$
5157.78	0.20		5157.75	0.03	$5d\ ^3D$–$7f$
5166.68 bl	0.4				$5f$–$7g$
5166.68 bl	0.4				$5g$–$7h$
5187.05	0.20		5187.07	−0.02	$5p\ ^3P$–$7s\ ^3S$
5217.82	0.200		5217.87	−0.05	$5p\ ^3P$–$7d\ ^3D$
5224.37	0.20		5224.35	0.02	$5d\ ^3D$–$7p\ ^3P$
5296.94	0.20				$5p\ ^1P$–$7s\ ^1S$
6142.01	0.05	3	6142.03	−0.02	$2s\ ^1S$–$2p\ ^1P$
6142.0024	0.0034	19			

[a] Beam-foil data. The remaining new lines are from JET spectra.
[b] Calculated from energy level values obtained from fitted Ritz formulae.
[c] Difference between observed and calculated energy values obtained from ELCALC, see text.

Table II. *Energy levels in Be III.*

Level	Energy (cm^{-1})	ΔE^a (cm^{-1})	N^b (cm^{-1})	O–R^c	n^*
$1s^2\,^1S$	0.0		5	0.0	
$2s\,^3S$	956 505.6	0.2	4	0.0	1.86236
$2s\,^1S$	981 175.4	0.5	2	0.0	1.94869
$3s\,^3S$	1121 186.2	0.9	4	0.0	2.86808
$3s\,^1S$	1127 702.9	5.1	1	1.0	2.94924
$4s\,^3S$	1175 298.1	0.8	2	0.2	3.86984
$4s\,^1S$	1177 926.6	6	1	0.3	3.94935
$5s\,^3S$	1199 613.1	0.6	2	−0.6	4.87057
$5s\,^1S$	1200 926.8	1.6	1	−1.5	4.94929
$6s\,^3S$	1212 592.8	4	1	0.6	5.87107
$6s\,^1S$	1213 340.7	7	1	−1.5	5.94924
$7s\,^3S$	1220 327.8	0.7	2	1.3	6.87146
$7s\,^1S$	1220 795.8	1.1	1	1.4	6.94965
$2p\,^3P_2$	983 373.5	0.3	4		
$2p\,^3P_1$	983 358.7	0.3	5		
$2p\,^3P_0$	983 370.2	0.3	4		
$2p\,^3P$	983 368.2	0.4	4	0.0	1.95695
$2p\,^1P$	997 452.2	0.5	5	0.0	2.01269
$3p\,^3P$	1128 302.2	0.7	4	−0.2	2.95705
$3p\,^1P$	1132 392.7	1.0	3	0.0	3.01210
$4p\,^3P$	1178 175.8	0.5	6	0.5	3.95714
$4p\,^1P$	1179 881.6	2.7	2	0.8	4.01177
$5p\,^3P$	1201 054.5	0.5	5	−0.3	4.95714
$5p\,^1P$	1201 922.2	0.8	3	−0.1	5.01154
$6p\,^3P$	1213 414.0	7	1	−1.1	5.95707
$6p\,^1P$	1213 931	60	1	16	6.01318
$7p\,^3P$	1220 839.6	0.5	1	−0.6	6.95710
$7p\,^1P$	1221 135	60	1	−19	7.00802
$3d\,^3D$	1131 381.0	1.0	9	−0.1	2.99820
$3d\,^1D$	1131 458.9	1.1	4	−0.3	2.99926
$4d\,^3D$	1179 454.2	0.5	9	0.2	3.99787
$4d\,^1D$	1179 498.3	0.6	5	0.4	3.99930
$5d\,^3D$	1201 703.8	0.4	5	−0.4	4.99768
$5d\,^1D$	1201 731.2	2.8	1	1.9	4.99941
$6d\,^3D$	1213 789.5	2.5	1	0.4	5.99767
$6d\,^1D$	1213 805.1	6	1	0.7	5.99937
$7d\,^3D$	1221 075.9	0.7	2	1.0	6.99774
$7d\,^1D$	1221 081.8	0.9	2	−3.1	6.99876
4f	1179 513.0	0.8	3	−0.4	3.99977
5f	1201 737.0	0.6	4	0.3	4.99978
6f	1213 810.8	1.2	4	2.3	5.99999
7f	1221 086.6	0.7	3	−0.8	6.99960
5g	1201 739.5	1.2	1	−0.1	4.99994
6g	1213 810.1	1.7	1	−0.2	5.99992
7g[d]	1221 086.4	1.4	1	−2.1	6.99957
9g	1229 050.9	4	1	−0.2	8.99989
7h	1221 088.9	2.2	1	0.1	7.00000

[a] Relative uncertainty. Absolute uncertainty is obtained by also including the ground state uncertainty (14 cm^{-1}).
[b] The number of observed combinations with this level.
[c] Difference between observed and Ritz calculated level values for *n*s, *n*p and *n*d series using the parameters in Table III. For *n*f, *n*g and *n*h series the difference was taken between observed values and those with the polarization formula with $E_l = 1\,241\,243.5 \pm 0.5$ cm^{-1}.
[d] Not included in the polarization formula because of a blend.

or to consider the center-of-gravity (CG) values of the singlet and triplet terms of each series. We have here preferred the second possibility as this to some extent cancels the interaction between ^1L_J and ^3L_J levels, although a weak G^1 (the exchange Slater integral) dependence remains. Unfortunately, all triplet terms but $2p\,^3P$ were unresolved. In 2p, for which the fine structure was resolved, the interaction between e.g. $2p\,^1P_1$ and $2p\,^3P_1$ depresses the latter level below $2p\,^3P_0$. For other members of the series the triplet term fine structures were not resolved but the interaction between the $^3P_1$ and $^1P_1$ levels remains throughout the series. For example, for the *n*s series the average mode is expressed by a two parameter formula instead of three parameters for the singlet and triplet branches. See Table III for a com-

Table III. *Ritz formulae for the* n*s,* n*p and* n*d series in Be III using the adopted ionization energy 1 241 243.5 cm^{-1}.*

Series	Ritz formulae
ns ^{3}S	$\delta = 0.128\,105 + 0.030\,173t + 0.010\,102t^2$
ns ^{1}S	$\delta = 0.050\,568 + 0.001\,010t + 0.006\,9285t^2$
ns	$\delta = 0.108738 + 0.029\,791t$
np ^{3}P	$\delta = 0.042\,755 + 0.002\,102t - 0.003\,763t^2$
np ^{1}P	$\delta = -0.011\,569 - 0.010\,4637t - 0.003\,763t^2$
np	$\delta = 0.029\,402 + 0.000\,571t$
nd ^{3}D	$\delta = 0.002\,574\,9 - 0.006\,966t$
nd ^{1}D	$\delta = 0.000\,694\,9 + 0.000\,350t$
nd	$\delta = 0.002\,085 - 0.004\,949t$

plete specification of the derived Ritz formulae. As a first step the ionization limit for the ns, np and nd series was fitted. The results 1 241 242.0, 1 241 243.2 and 1 241 243.4 cm^{-1}, respectively, are quite satisfactory. The average ionization energy value from these analyses was determined to 1 241 243.2 $\pm$ 0.5 cm^{-1}. In order to achieve an ionization limit on an absolute scale we have to add the ground state uncertainty of 14 cm^{-1}. In the next step the derived ionization limit was implemented in the Ritz formula for each triplet and singlet branch of the ns, np and nd series. The differences between observed and the Ritz-calculated energy level values are included in Table II. As expected, the largest deviations were found for the np ^{1}P series, because these energy level values have been obtained from measurements at short wavelengths in the XUV region.

4.2.2. *The polarization formula.* A useful and sensitive method for ionization limit determination is the polarization formula applied to hydrogenic term values, $T_{n,l}$ which can be written as:

$$T_{n,l} = \zeta^2 R_{\mathrm{Be}}/n^2 + \Delta_{\mathrm{r}} + \Delta_{\mathrm{p}} \tag{3}$$

where

$$\Delta_{\mathrm{p}} = \zeta^4 \alpha_{\mathrm{d}} P(n,l)[1 + \zeta^2 \alpha_{\mathrm{q}}/\alpha_{\mathrm{d}} q(n,l)] \tag{4}$$

and

$$\Delta_{\mathrm{r}} = R_{\mathrm{Be}} \alpha^2 \zeta^4 n^{-4}[n/(1+1/2) - 3/4]. \tag{5}$$

Here P and q are functions of quantum numbers n and l, tabulated by Edlén [28]. The hydrogenic dipole and quadrupole polarizabilities for He-like ions have been calculated by Dalgarno [29] yielding the values $\alpha_{\mathrm{d}} = 9/2Z^4$ and $\alpha_{\mathrm{q}} = 15/Z^6$. However, it has been shown that in the Be III case these theoretical values cannot be applied to the nd levels [2,3] and our results confirm this. Thus, we find that the observed 3d, 4d, 5d and 7d term values are 12.3, 8.7, 5.5 and 2.6 cm^{-1} smaller than the corresponding theoretical values. On the other hand, agreement is good with theory for the 4f, 5f, 6f and 7f levels where the differences are as low as −0.3, −1.1, −3.1 and 0.0 cm^{-1} respectively. Note also that the hydrogenic core polarizabilities given after Eq. (4) include only the adiabatic portion of the interaction. There is also a non-adiabatic correlation, see e.g. Curtis [30]. We have determined the experimental ionization energy by including only the dipole polarizability in the polarization formula. The quadrupole parameter was found to be extremely small and was therefore neglected. All but 7g of our observed hydrogenic configurations were included in the polarization formula. The ionization energy was observed at 1 241 243.7 $\pm$ 0.6 cm^{-1}. This value is close to that obtained with the Ritz formula on the s, p and d series. The final ionization energy is an average value of the fitting procedures using the Ritz and polarization formulas, deduced to 1 241 243.5 $\pm$ 0.6 cm^{-1}.

5. Comparison with theory

Comparisons of experimental and theoretical data for He-like ions are primarily motivated by the determination of the effects of quantum electrodynamics, QED. These are largest for the ns ^{1,3}S states and scale approximately as n^{-3}. By comparing the experimental 1s^2 ^{1}S$_0$ ionization energies with the calculated ones the QED contribution ("Lamb shift") can be obtained [1–7]. In the Be III case our experimental ionization energy equals 1 241 243.5 $\pm$ 14 cm^{-1}. This value practically coincides with that given by Löfstrand [3], 1 241 242 $\pm$ 15 cm^{-1}. Thus, the new lines identified in the present work have not changed the value of the ionization limit. The uncertainty is mainly caused by that in the 1s^2 ^{1}S$_0$-1s2p ^{1}P$_1$ resonance line [17]. These experimental results can be compared with the theoretical value which includes QED, 1 241 256.601 cm^{-1} [9]. The difference 14 cm^{-1} is as large as the experimental uncertainty. The QED contribution [9] is −29.996 cm^{-1}, in agreement with the experimental QED part -43 ± 14 cm^{-1}. We may note that an earlier QED calculations gives a similar result, −28.6 cm^{-1} [31].

It is clear that our experimental uncertainty is too crude for a detailed test of theory. For the 1s2s ^{1}S and 1s2s ^{3}S levels in Be III precise experimental tests of QED contributions are provided by the fast-ion-beam laser studies [19,20] which are sufficiently accurate to even test higher-order QED effects. The theoretical QED contributions are here −2.9 cm^{-1} (^{1}S) and −3.6 cm^{-1} (^{3}S), see Drake [9].

In Table IV we have listed a number of experimental and theoretical term values. Notice that all experimental term values ($n = 2$ and higher) are tightly connected with relative uncertainties of less than 1 cm^{-1}, whereas their uncertainties with respect to the ground state, or absolute uncertainties, are larger ($\pm$14 cm^{-1}). This will of course reflect the residuals in Table IV. For 2s ^{1}S, 2p ^{1}P, 2s ^{3}S and 2p ^{3}P, for example, we note differences of 3.2, 3.1, −3.5 and −3.5 cm^{-1}, respectively, between our observed values and theory [9]. This means that our observed and theoretical energy differences of 2s ^{1}S–2p ^{1}P and 2s ^{3}S–2p ^{3}P are practically coinciding, giving observed QED corrections of -2.9 ± 0.1 and -4.2 ± 0.2 cm^{-1} for these intervals, respectively. However, as noted above, these data are now superseded by the beam-laser studies [19,20].

The observed $n = 4$ and 5 states listed in Table IV, are compared with the relativistic calculations by Accad *et al.* [18]. The Lamb shift of 4s should according to the n^{-3} scaling law be below 0.5 cm^{-1} and this is within the experimental error bars. The agreement is very good as can be seen in Table IV. The largest deviation is found for 4s ^{3}S (−2.7 cm^{-1}). Another quantity of interest for comparison is the 2p ^{1}P–2p ^{3}P splitting because the theoretical term values by Accad *et al.* [18] were used in the previous studies [2,3].

Table IV. *Comparison of experimental and theoretical term values in Be III, (in cm^{-1}).*

Level	T_{exp}	T_{th}	$\Delta(T_{\mathrm{exp}} - T_{\mathrm{th}})$
$1s^2\,{}^1S$	1 241 243.5	1 241 256.6[a]	−13.1
$2s\,{}^1S$	260 068.1	260 064.3[a]	3.8
$3s\,{}^1S$	113 540.6	113 540.0[b]	0.6
$5s\,{}^1S$	40 316.7	40 316.0[c]	0.7
$2s\,{}^3S$	284 737.9	284 740.8[a]	−2.9
$3s\,{}^3S$	120 057.3	120 060.3[c]	−3.0
$4s\,{}^3S$	65 945.4	65 947.5[c]	−2.1
$5s\,{}^3S$	41 630.4	41 631.0[c]	0.6
$2p\,{}^1P$	243 791.3	243 787.6[a]	3.7
$3p\,{}^1P$	108 850.8	108 853.2[b]	−2.4
$4p\,{}^1P$	61 361.9	61 362.6[c]	−0.7
$5p\,{}^1P$	39 321.3	39 320.7[c]	0.6
$2p\,{}^3P$	257 875.3	257 878.2[a]	−2.9
$3p\,{}^3P$	112 941.3	112 943.2[b]	−1.9
$4p\,{}^3P$	63 067.7	63 068.7[c]	−1.0
$5p\,{}^3P$	40 189.0	40 188.9[c]	0.1
$3d\,{}^3D$	109 862.5	109 856[d]	6.5
$4d\,{}^3D$	61 789.3	61 785[e]	4.3
$5d\,{}^3D$	39 539.7	39 534[e]	5.7
$3d\,{}^1D$	109 784.6	109 774[d]	10.6
$4d\,{}^1D$	61 445.2	61 738[e]	7.2
$5d\,{}^1D$	39 512.3		
4f	61 730.5	61 728.3[f]	2.2
5f	39 506.5	39 505.0[f]	1.5

[a] Drake [9].
[b] Drake [10].
[c] Accad *et al.* [18].
[d] Brown [34].
[e] Brown and Cortez [35].
[f] Brown [33].

Our observed splitting is 14 084.0 cm^{-1}, while theories predict 14 087.50 cm^{-1} [18] or 14 090.6 cm^{-1} [9].

For the *n*d and *n*f states we have compared our data with the non-relativistic calculations by Brown and Cortez [33–35]. The differences between observed and calculated values here exceed the experimental error bars of which those for the singlet levels are largest. The observed singlet-triplet splitting of nd levels for C V has been discussed by Engström *et al.* [5]. Their data for the (^1D–^3D) splitting were in agreement with the calculations by Chang [36]. The l and Z dependent singlet and triplet splitting caused by electrostatic exchange and spin–orbit interactions was expressed as:

$$n\mathrm{d}(^3D - {}^1D) = a/n^3 + b/n^5 + c/n^7. \qquad (6)$$

With $a = 3750$, $b = -14\,800$ and the last term being ignored all *n*d (^3D–^1D) splittings in Be III are reproduced within the error bars.

6. Isoelectronic comparisons

The experimental value of the Be III $1s^2\,{}^1S$ Lamb shift, -43 ± 14 cm^{-1}, agrees with the theoretical values as discussed above. However, the experimental uncertainty is quite substantial and no real checks of theory can therefore be made. It is interesting to compare with the situation for other He-like systems.

For B IV and C V the experimental $1s^2\,{}^1S$ Lamb shifts are -93 ± 20 cm^{-1} [4] and -166 ± 20 cm^{-1} [5], respectively, to be compared with Drake's theoretical values -73.636 cm^{-1} and -150.279 cm^{-1} [9]. As mentioned above, the experimental uncertainties are mostly caused by the wavelength uncertainty for the $1s^2\,{}^1S$–$1s2p\,{}^1P$ resonance line. For N VI and O VII this transition was re-measured using laser-produced plasmas [37]. The uncertainties thereby established are about 5 times lower than for earlier experimental data. Using these new results, published data for N VI [6] and O VII [7] as well as unpublished data for these spectra, Engström, Kink, *et al.* [38,39] report the values -313 ± 27 cm^{-1} (N VI) and -505 ± 75 cm^{-1} (O VII). The theoretical corresponding results are -271.396 and -449.309 cm^{-1} [9].

Kink [39] also mentions the possibility of a small significant systematic discrepancy between theory and experiment, but he also adds that the new experimental value for O VII is somewhat preliminary. Indeed, the value given by Isler *et al.* [7], -440 ± 175 cm^{-1}, agrees with theory although the uncertainty is larger than for the latest value. In an investigation of X-ray transitions ($1s^2\,{}^1S$–$1s2p\,{}^1P$) in tokamak spectra for He-like K, Sc, Ti, V, Cr, Fe and Kr [$Z = 19$–36]. Beiersdorfer *et al.* [40] also found similar systematic differences between theoretical and experimental data. On the other hand, more recent measurements using an EBIT (electron beam ion trap) for He-like Ge, Xe, Dy, W, Os and Bi ($Z = 32$–83) by Marrs *et al.* [41], are in very satisfactory agreement with theoretical QED calculations [42,43]. It thus appears that additional experimental work is needed for several He-like systems.

7. Conclusion

Inspired by the plasma diagnostic activity at JET involving beryllium, we have performed a spectroscopic investigation of Be III. The results have been complemented by studies of beam-foil spectra. Together with C V [1,5] the spectrum Be III is now one of the most thoroughly studied among He-like ions.

Acknowledgements

We are grateful to Professor L.J. Curtis for valuable comments on the manuscript. The work has been supported by the Swedish Natural Science Council (NFR). One of the authors (CJ) is grateful for the hospitality during his stays at JET.

References

1. Edlén, B. and Löfstrand, B., J. Phys. B: At. Mol. Phys. **3**, 1380 (1970).
2. Eidelsberg, M., J. Phys. B: At. Mol. Phys. **5**, 1031 (1972).
3. Löfstrand, B., Physica Scripta **8**, 57 (1973).
4. Eidelsberg, M., J. Phys. B: At. Mol. Phys. **7**, 1476 (1974).
5. Engström, L., Bengtsson, P., Jupén, C. and Westerlind, M., J. Phys. B: At. Mol. Opt. Phys. **25**, 2459 (1992).
6. Malvezzi, A. M., Physica Scripta **27**, 413 (1983).
7. Isler, R. C., Jupén, C. and Martinson, I., Physica Scripta **47**, 32 (1993).
8. Martin, W. C., Physica Scripta **24**, 725 (1981).
9. Drake, G. W., Can. J. Phys. **66**, 586 (1988).
10. Drake, G. W. F., unpublished data (1985).

11. Cheng, K. T., Chen, M. H., Johnson, W. R. and Sapirstein, J., Phys. Rev. A **50**, 247 (1994).
12. Ericson, A. and Edlén, B., Z. Physik **59**, 656 (1930).
13. Edlén, B., Nature **127**, 405 (1931).
14. Edlén, B., Phys. Rev. **44**, 778 (1933).
15. Kruger, P. G. and Cooper, F. S., Phys. Rev. **44**, 418 (1933).
16. Robinson, H. A., Phys. Rev. **51**, 14 (1937).
17. Svensson, L. Å., Physica Scripta **1**, 246 (1970).
18. Accad, Y., Pekeris, C. L. and Schiff, B., Phys. Rev. A **4**, 516 (1971).
19. Scholl, T. J., Holt, R. A. and Rosner, S. D., Phys. Rev. A **39**, 1163 (1989).
20. Scholl, T. J. *et al*., Phys. Rev. Lett. **71**, 2188 (1993).
21. Boileau, A. *et al*., Plasma Phys. Contr. Fusion **31**, 779 (1989).
22. Jupén, C. *et al*., Physica Scripta, 563 (2001).
23. Engström, L., Lund Reports on Atomic Physics, LRAP-232 (1995).
24. Mannervik, S., Martinson, I. and Jelenkovic, B., J. Phys. B: At. Mol. Phys. **14**, L275 (1981).
25. Andersen, T., Bentzen, S. M. and Poulsen, O., Physica Scripta **22**, 119 (1980).
26. Summers, H. P. *et al*., JET Report, JET-P (91) 12.
27. Radziemski, L., Fischer, K. J., Steinhaus, D. W. and Goldman, A. S., Comput. Phys. Commun. **3**, 9 (1973).
28. Edlén, B., in ''Handbuch der Physik Vol. 27'' (Edited by S. Flügge), (Springer, Heidelberg, 1964), pp. 80–204.
29. Dalgarno, A., Adv. Phys. **11**, 281 (1962).
30. Curtis, L. J., Physica Scripta **35,** 805 (1987).
31. Ermolaev, A., M. Phys. Rev. A **8**, 1651 (1973).
32. Pekeris, C. L., Phys. Rev. **126**, 143 (1962).
33. Brown, R. T., Astrophys. J. **158**, 829 (1969).
34. Brown, R. T., J. Chem. Phys. **48**, 4698 (1968).
35. Brown, R. T. and Cortez, J.-L., J. Chem. Phys. **54**, 2657 (1971).
36. Chang, T. N., J. Phys. B: At. Mol. Phys. **7**, L108 (1974).
37. Engström, L. and Litzén, U., J. Phys. B: At. Mol. Opt. Phys. **28**, 2565 (1995).
38. Engström, L. *et al*., unpublished work.
39. Kink, I., Doctoral Dissertation, Lund University (1999).
40. Beiersdorfer, Bitter, M., von Goeler, S. and Hill, K. W., Phys. Rev. A **40**, 150 (1989).
41. Marrs, R. E., Elliott, S. R. and Stöhlker, Th., Phys. Rev. **52**, 3577 (1995).
42. Mohr, P. J., Plunien, G. and Soff, G., Phys. Reports **293**, 227 (1998).
43. Persson H., Salomonson, S., Sunnergren, P. and Lindgren, I., Phys. Rev. Lett. **76**, 204 (1996).

